17 April 2000

PHYSICS LETTERS A

Physics Letters A 268 (2000) 209–216

www.elsevier.nl/locate/physleta

Neutron polarimetric separation of geometric and dynamical phases

A.G. Wagh [a], G. Badurek [b,*], V.C. Rakhecha [a], R.J. Buchelt [b], A. Schricker [b]

[a] *Solid State Physics Division, Bhabha Atomic Research Centre, Mumbai, India*
[b] *Institute of Nuclear Physics, University of Technology, Stadionallee 2, 1020 Vienna, Austria*

Received 1 November 1999; received in revised form 8 March 2000; accepted 16 March 2000
Communicated by P.R. Holland

Abstract

We present a neutron polarimetric experiment clearly demarcating geometric and dynamical phases. Here a relative rotation between two identical π spin flippers produces a pure geometric phase and their relative translation yields a pure dynamical phase. The experiment agrees with theory to within about 1%. © 2000 Elsevier Science B.V. All rights reserved.

Keywords: Geometric phase; Neutron polarimetry; Spinor phase

On a revisit to the quantum adiabatic theorem, Berry [1] discovered a Hamiltonian-independent, nonintegrable phase component, generally ignored in the theorem. This geometric phase was subsequently found to arise in completely general, e.g. nonadiabatic [2], noncyclic [3] or nonunitary [4] evolutions of a quantal system. It was also realized that Pancharatnam [5] had explicitly recognized geometric phase in its general form about three decades earlier, while studying interference between optical beams of distinct polarizations. Geometric phase depends only on the geometry of the curve traced in the projective Hilbert, or ray, space [6,7] and equals the phase anholonomy of a parallel transported wavefunction. Geometric phase has since been discerned [8–12] in a wide range of scientific disciplines.

Neutron quantum beats, observed interferometrically by Badurek et al. [13] and attributed by Wagh and Rakhecha [14,15] to a time-proportional geometric phase, represent an early measurement of geometric phase. Tomita and Chiao [16] propagated linearly polarized light along a coiled optical fibre and measured the concomitant rotation of polarization, arising from the equal and opposite adiabatic geometric phases acquired by the constituent right and left circular polarization states. The neutron polarimetric analogues [17,18] of this experiment, however, had to discern the geometric phase from the much larger dynamical phase characteristic of the adiabatic evolutions. An ideal geometric phase experiment should eliminate dynamical phase by parallel transporting a

* Corresponding author. Tel. +43-1-72701-229; fax: +43-1-58801-14199.
E-mail address: badurek@ati.ac.at (G. Badurek).

PII: S0375-9601(00)00211-5

quantal system [7] or implementing an evolution with a net null dynamical phase [14,19–21]. Wagh [19] proposed a neutron experiment to observe the spinor phase dependence on the orientation of the precession axis. Wagh and Rakhecha [14] subsequently showed that this experiment demarcated geometric and dynamical phases. In this Letter, we present a neutron polarimetric observation of clearly separated geometric and dynamical phases.

We consider a region permeated by a uniform magnetic induction $\boldsymbol{B}_0 = B_0\hat{\boldsymbol{z}}$ in which a $|z\rangle$-polarized neutron beam propagating with a velocity $\boldsymbol{v}_0 = v_0\hat{\boldsymbol{x}}$ successively encounters (Fig. 1) two identical spin flippers F_1 and F_2. The flipper F_1 (F_2) precesses the neutron spin through 180° about a predetermined direction in the xy-plane at an angle β_1 (β_2) to the y-axis. Within the flipper F_1, the neutron spin $\boldsymbol{s}$ traces a semi-great circle from $\hat{\boldsymbol{z}}$ to $-\hat{\boldsymbol{z}}$ on the unit sphere of spin directions (Fig. 2). Between the flippers F_1 and F_2, the $-\hat{\boldsymbol{z}}$ spin precesses through an angle $\phi_\downarrow$ about the guide field $B_0\hat{\boldsymbol{z}}$. The flipper F_2 returns the $-\hat{\boldsymbol{z}}$ spin to the initial direction $\hat{\boldsymbol{z}}$ along another semi-great circle. The two semi-great circles enclose an angle $\beta_1 - \beta_2 + \pi$ and hence a solid angle $-2(\beta_1 - \beta_2 + \pi)$. The neutron spin $\hat{\boldsymbol{z}}$ then precesses about $B_0\hat{\boldsymbol{z}}$. The total precession in the $|+z\rangle$ state, viz. the sum of precessions before entering F_1 and after exiting F_2, equals $\phi_\uparrow$. Since the initial and final spin states are identical,

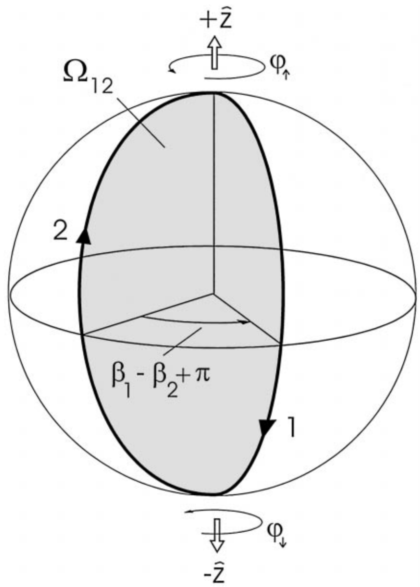

Fig. 2. The spin curve for an incident $|+z\rangle$ state traversing identical π flippers F_1 and F_2 whose horizontal fields $\boldsymbol{B}_1$ are oriented at angles β_1 and β_2 respectively to $\hat{\boldsymbol{y}}$. Semi-great circles **1** and **2** traced within F_1 and F_2 respectively enclose a solid angle $\Omega_{12} = -2(\beta_1 - \beta_2 + \pi)$ resulting in a geometric phase equal to $\beta_1 - \beta_2 + \pi$. Between F_1 and F_2, the spin $-\boldsymbol{z}$ precesses by $\phi_\downarrow$ about the guide field; the spin $+\boldsymbol{z}$ precesses by a total angle $\phi_\uparrow$ over the regions $R_1 \to F_1$ and $F_2 \to R_2$ (cf. Fig. 1). These precessions generate a dynamical phase equal to $(\phi_\downarrow - \phi_\uparrow)/2$.

viz. $|z\rangle$, this spinor evolution is cyclic. A rotation $\delta\beta$ of F_1 relative to F_2 about the $\hat{\boldsymbol{z}}$ direction, changes

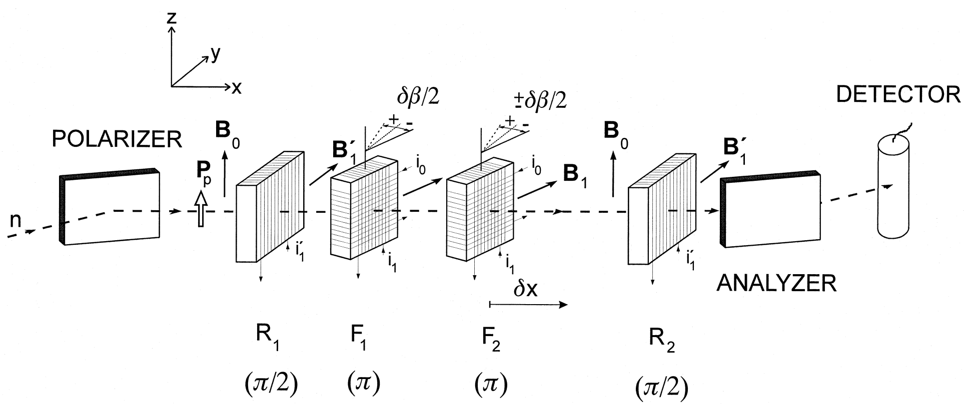

Fig. 1. Schematic sketch of the experiment. A uniform guide field $B_0\hat{\boldsymbol{z}}$ is applied over the setup. The incident neutron beam is $|z\rangle$-polarized by the supermirror polarizer. F_1 and F_2 are identical π flippers for the $\hat{\boldsymbol{z}}$ spin. For an incident $|z>$ state, a relative rotation $\delta\beta$ between F_1 and F_2 about $\hat{\boldsymbol{z}}$ produces a pure geometric phase $\Phi_G = \delta\beta$; a translation δx of F_2 results in a proportionate pure dynamical phase Φ_D (cf. Eqs. (1), (2)). For a polarimetric measurement of these phases, the $\pi/2$ flipper R_1 converts the $|z\rangle$ state to $|y\rangle$ and the second $\pi/2$ flipper R_2 projects the local $|y\rangle$ component back to $|z\rangle$ for a spin polarization analysis.

the solid angle by $\Omega = -2\delta\beta$ generating a pure geometric phase

$$\Phi_G = -\frac{\Omega}{2} = \delta\beta\,, \tag{1}$$

which stems directly from the angle anholonomy Ω for a parallel transported vector, $\boldsymbol{s}$ here, on a 2-sphere.

A translation δx of F_2 along the beam direction on the other hand, increases $\phi_\downarrow$ by $\delta\phi = 2|\mu|B_0\delta x/\hbar v_0$ and reduces $\phi_\uparrow$ by the same amount, but leaving the spin curve and hence its solid angle unaltered. Here μ denotes the magnetic moment of the neutron. The translation δx therefore results in a pure dynamical phase

$$\Phi_D = \frac{\delta\phi_\downarrow - \delta\phi_\uparrow}{2} = \delta\phi = \frac{2|\mu|B_0\delta x}{\hbar v_0}\,. \tag{2}$$

In contrast to the geometric phase which depends only on the geometry of the (spin) curve traced in the ray space, the dynamical phase, being proportional to the time integral of $\boldsymbol{B}\cdot\boldsymbol{s}$, depends on the Hamiltonian and is integrable.

There are two well-known strategies to observe phases. In the first, viz. 'two-Hamiltonian, one-state' strategy [9], the phases are determined interferometrically. In the other, 'one-Hamiltonian, two-state' strategy [16–18,22], a coherent superposition of two orthogonal states, $|z\rangle$ and $|-z\rangle$ here, is subjected to the single Hamiltonian. At the end of a cyclic evolution for the $|z\rangle$ and $|-z\rangle$ states producing phases Φ_+ and Φ_- respectively, the final spin differs from the initial spin by a rotation equal to $\Phi_- - \Phi_+$ about $\hat{\boldsymbol{z}}$.

For neutrons, this polarimetric phase measurement has several advantages over interferometry. Neutron polarimetry is insensitive to ambient mechanical and thermal disturbances. It is also free from spatial constraints imposed by small perfect crystal interferometers. In an interferometric experiment, the perfect crystal interferometer accepts neutrons incident within an angular range of only a few arcseconds at each neutron wavelength, thus reducing the usable neutron intensity by about 3 orders of magnitude. A polarimetric measurement on the other hand, uses a substantial fraction of the incident neutron intensity and hence can be carried out even at a low-flux reactor. Furthermore, here both the orthogonal states comprised in each neutron acquire identical scalar phases which therefore get eliminated in the resultant spin rotation, providing a clean SU(2) phase measurement. The polarimetric experiment of Badurek et al. [23] could thus observe scalar Aharanov-Bohm phases with a white neutron beam and establish their nondispersivity. The only limitation of a polarimetric experiment is its modulo 180° phase measurement, since the two orthogonal states acquire equal and opposite SU(2) phases Φ_+ and Φ_-. In the present experiment however, this modulo 180° phase determination does not lead to any loss of information.

The experiment was carried out at the tangential beam port of the 250 kW *TRIGA* research reactor of the Atominstitut of the Austrian Universities in Vienna. A schematic sketch of the setup is shown in Fig. 1. A neutron beam from a pyrolitic graphite monochromator (omitted in Fig. 1) with a mean wavelength λ_0 of 1.96 Å is polarized vertically upwards, i.e. along $+\hat{\boldsymbol{z}}$, by a reflection from a bent Co–Ti supermirror array. The 5 mm wide and 10 mm high polarized beam traverses a path-length of 600 mm in a uniform vertical magnetic guide field $\boldsymbol{B}_0$. In the central region, where two identical DC spin flippers F_1 and F_2 are located, the field strength measured with a Hall probe is 13.9 ± 0.2 G. The $|+z\rangle$ fraction of the beam is analyzed by a second supermirror. Each flipper consists of a pair of rectangular coils of anodized Al wire (diam. 0.75 mm) wound directly one upon the other at right angles around a fibre-glass frame of dimensions $60 \times 60 \times 25$ mm^3 with a central hole of 35 mm diameter for beam passage. The inner coil produces a horizontal field $\boldsymbol{B}_1$ whereas the outer one serves to compensate the guide field by producing an equal and opposite vertical field. When aligned perpendicular to the beam both flippers yielded a flipping ratio of 24.3 ± 1.0 at a field $B_1 = 13.6 \pm 0.2$ G, which is in agreement with the calculated field for 1.96 Å neutrons traversing an effective path-length of 25.5 mm. If the flipper F_1 (F_2) precesses the neutron spin through an angle θ_1 (θ_2), the $|+z\rangle$-intensity behind the analyzer is proportional to $1 + P_p P_a[\cos\theta_1\cos\theta_2 - \sin\theta_1\sin\theta_2\cos\phi_\downarrow]$. Here P_p and P_a are the polarizations produced in the polarizer and analyzer respectively. The $|+z\rangle$-intensities I_{++}, I_{+-}, I_{-+} and I_{--} measured with the respective flippers 'on' ($_-$) or 'off' ($_+$), yield a flipping efficiency of 100% for either flipper ($\theta_1 = \theta_2 = 180°$, with flipper on) within experimental errors and polarizations $P_p = P_a = 0.960 \pm 0.0016$. Both flippers can be rotated independently of each other about the vertical axis in an angular range $-38° \leq \delta\beta/2 \leq +38°$. Flipper F_2 can be displaced downstream from its initial position (50 mm behind flipper F_1) by a distance $0 \leq \delta x \leq 60$ mm.

The current-carrying coil R_1 (Fig. 1) in conjunction with the guide field functions as a $\pi/2$ flipper to take the incident $|z\rangle$ state to $|y\rangle$, a coherent superposition of $|z\rangle$ and $|-z\rangle$ in equal proportions. The coil R_1 produces a field $B_1' = B_0$ along $+\hat{\boldsymbol{y}}$. The resultant field of magnitude $\sqrt{2}B_0$ inside the coil directed along the bisector of $\hat{\boldsymbol{y}}$ and $\hat{\boldsymbol{z}}$ axes is adjusted to generate exactly half a Larmor precession during the neutron passage time through the coil. The initial spin vector $+\hat{\boldsymbol{z}}$ is hence rotated to $+\hat{\boldsymbol{y}}$. The second $\pi/2$ flipper R_2, identical to R_1, converts the local $+\hat{\boldsymbol{y}}$-component of the polarization back to the $+\hat{\boldsymbol{z}}$ component for the analyzing supermirror. The distance between these two $\pi/2$ flippers of about 45 cm was kept constant throughout the experiment.

The incident neutron beam had a spread $\Delta\lambda/\lambda_0 = \Delta v/v_0 \simeq 0.023$ in wavelength and velocity as determined by time-of-flight spectroscopy. Due to the consequent spread in the neutron passage time through R_1, not all neutrons incident in the $|z\rangle$ state emerged $|y\rangle$-polarized. The net $|y\rangle$-polarization after the flipper R_1 was therefore less than the incident $|z\rangle$-polarization P_p by a depolarization factor $D_R = 0.9996$. A similar depolarization took place within R_2. Again, the nominal path-length of about 40 cm between R_1 and R_2 corresponds to about 8 full Larmor cycles of the polarization vector about the guide field, which for the given wavelength spread implies an additional depolarization factor $D = 0.79$. Hence at the detector, a net polarization $\tilde{P} = P_p D_R D D_R P_a = 0.73 \pm 0.02$ is attained.

The geometric and dynamical phase shifts, produced by a relative rotation and translation respec-

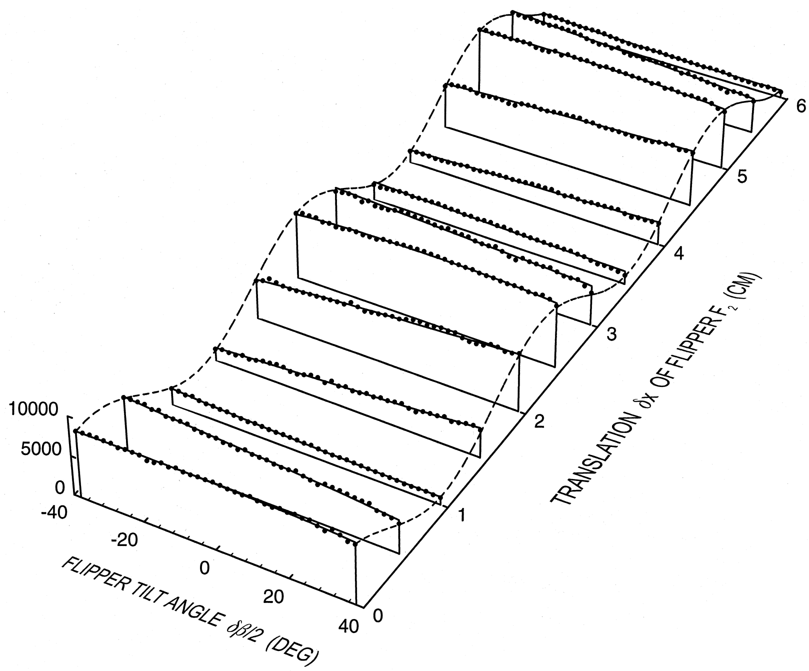

Fig. 3. Measured intensity I_{yy} for parallel rotation of flippers F_1 and F_2 by an angle $\delta\beta/2$ for a series of downstream displacements δx of the flipper F_2. The full and the dashed curves represent least-squares fits to the data according to Eq. (6).

tively between the flippers F_1 and F_2, could be derived via the associated polarization change by monitoring the intensity

$$I_{yy} \propto 1 + \tilde{P}\cos\left\{2\left[\Phi_G\left(\frac{\delta\beta}{2}\right) + \Phi_D(\delta x) + \Phi_0\right]\right\}, \tag{3}$$

as a function of the flipper rotations $\delta\beta/2$ and F_2 translations δx. The symbol Φ_0 stands for the phase acquired with $\delta\beta/2 = 0$ and $\delta x = 0$.

Two different sets of I_{yy} spectra were recorded. For the first set, both flippers were rotated by $\delta\beta/2$ in the *same* direction (Fig. 1) in steps of 2° from $-38°$ to $+38°$ for 13 different translations δx of the flipper F_2. For each angular position, the flipper currents i_1 were readjusted to compensate for the $1/\cos(\delta\beta/2)$-dependence of their effective thickness, so as to maintain the π spin flip in each flipper. Since the two flippers remained parallel throughout this set, we expect a null geometric phase (Eq. (1)) here. The results of this experiment are shown in Fig. 3.

The second set of intensity patterns was obtained for flipper rotations $\delta\beta/2$ in *opposite* directions, producing a geometric phase equal to $\delta\beta$. This set is plotted in Fig. 4. Here the intensity oscillates with variations in both $\delta\beta/2$ and δx as predicted. The observed I_{yy} oscillations exhibit a visibility close to $\tilde{P} = 0.73$ in accordance with Eq. (3).

Ideally, one would not expect any variation of the detected intensity for parallel rotation of the flippers, since for a fixed displacement δx, neither the geometric nor the dynamical phase should change. The observed patterns however, do display a small intensity variation (Fig. 3) with $\delta\beta$. This variation can arise from small y-displacements Δy_1 and Δy_2 of rotation axes of the two flippers from the beam centre. The flipper rotations would then displace the flippers by $\delta x_j = \Delta y_j \tan(\delta\beta/2)$, $j = 1,2$ along the beam direction, generating a corresponding net dynamical phase $\Delta\Phi_D$ in accordance with Eq. (2). Due to the relatively large guide field used here, this contamination can become significant in comparison with the small geometric phase ($= 0$ and $\delta\beta$ respectively) expected for the two sets, even with offsets Δy_j of about 1 mm. Similarly, a tiny misalignment

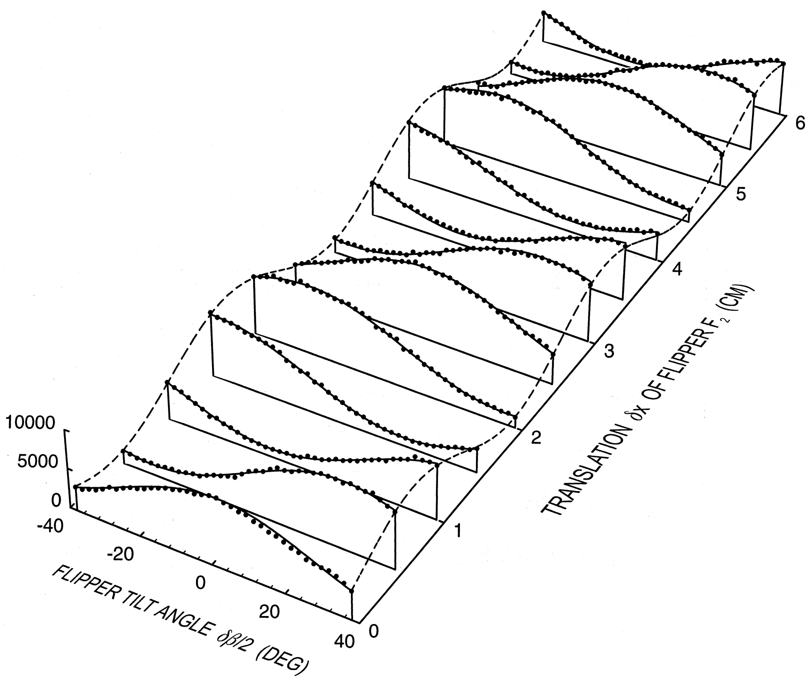

Fig. 4. Same as Fig. 3 but with the two flippers rotating in opposite directions.

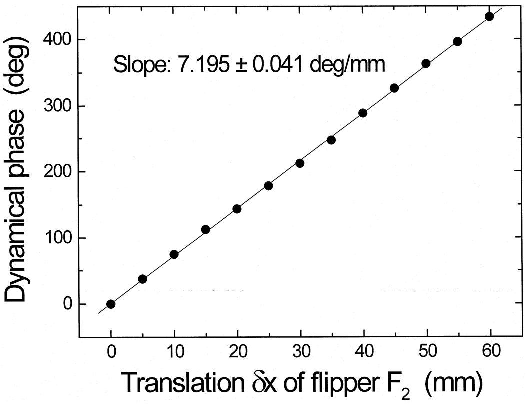

Fig. 5. Pure dynamical phase Φ_D as a function of the translation δx of flipper F_2. Error bars are smaller than the size of points. The straight line is the best fit to the data. Its slope matches that expected for the measured guide field.

ϵ, of the order of 1°, between the directions of F_2 translation and beam propagation, can change the lateral offset of F_2 by $\delta x \sin\epsilon$ and x-translation of F_2 to $\delta x \cos\epsilon$. These departures from ideality in the experiment would therefore introduce a dynamical phase contamination

$$\Delta\Phi_D(\delta\beta,\delta x) = \frac{2|\mu|B_0}{\hbar v_0}\{\pm[\Delta y_2 + \delta x \sin\epsilon] - \Delta y_1\}\tan\frac{\delta\beta}{2}, \tag{4}$$

to the geometric phase (Eq. (1)). The + and − signs of ± in this equation apply for parallel and opposite rotations, respectively, of the two flippers. The dynamical phase will be similarly modified to

$$\Phi_D(\delta x) = \frac{2|\mu|B_0}{\hbar v_0}\delta x \cos\epsilon. \tag{5}$$

Therefore the intensity behind the analyzer is expected to vary with simultaneous rotations of F_1 and F_2 and the translation of F_2 according to

$$I_{yy}(\delta\beta,\delta x) \propto 1 + \tilde{P}\cos\left\{2\left[k\left(\frac{\delta\beta}{2} \mp \frac{\delta\beta}{2}\right) + \Phi_D(\delta x) + \Delta\Phi_D(\delta\beta,\delta x) + \Phi_0\right]\right\}. \tag{6}$$

The − and + signs of ∓ here apply for parallel and opposite rotations respectively, of the two flippers. The parameter k has been introduced to measure the deviation between the observed and theoretical geometric phases.

A least-squares fit to the observed intensity variations yielded the following values of the parameters:

1. $2|\mu|B_0/\hbar v_0 = 7.199 \pm 0.08$ deg/mm, implying a guide field $B_0 = 13.84 \pm 0.16$ G which agrees well with its measured value of 13.9 ± 0.2 G.
2. The initial phase $\Phi_0 = -363 \pm 1.6$ deg, close to the phase calculated for the difference $x(R_1 \to F_1) + x(F_2 \to R_2) - x(F_1 \to F_2)$ between the path-lengths for the unflipped and flipped spin states at $\delta x = 0$.
3. The misalignment angle $\epsilon = 1.86 \pm 0.32$ deg
4. $\Delta y_1 = -1.79 \pm 0.21$ mm
5. $\Delta y_2 = -0.15 \pm 0.21$ mm and
6. $k = 0.986 \pm 0.006$, derived from the second set of intensity patterns measured for opposite rotations $\delta\beta/2$ of the two flippers.

The dynamical phase variation with the translation δx of F_2, derived from the opposite rotation data, is shown in Fig. 5. A linear fit yields a slope of 7.195 ± 0.041 deg/mm, corresponding to a guide

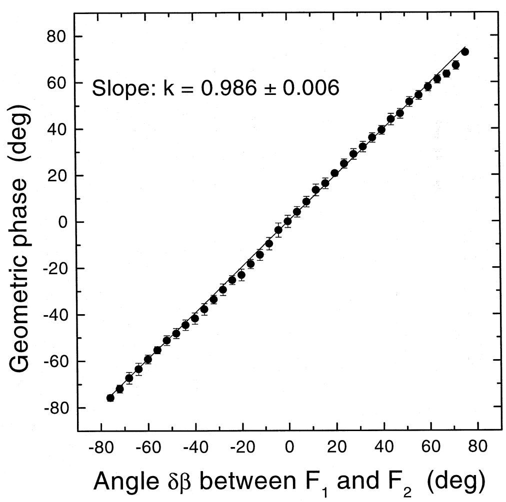

Fig. 6. Observed geometric phase as a function of the angle $\delta\beta$ between the flippers F_1 and F_2. The straight line is the best fit to the data.

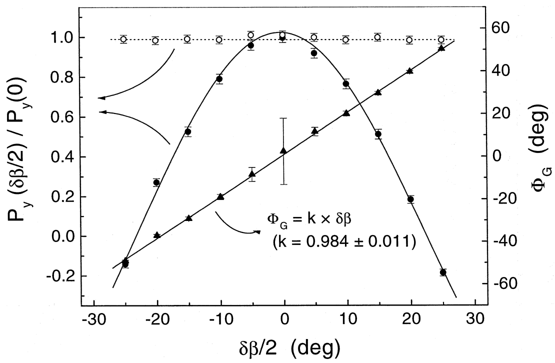

Fig. 7. Measured normalized polarization $P_y(\delta\beta/2)/P_y(0)$ for parallel (○) and opposite (●) rotations $\delta\beta/2$ of flippers F_1 and F_2, mounted in a field-free region within a soft magnetic shielding. The phases derived from the parallel- and opposite- (shown by filled triangles) rotation data without applying any corrections conform well to the theoretical geometric phases equal to 0 and $\delta\beta$ respectively. Curves through the data points represent the best fits.

field of 13.84 ± 0.07 G (cf. Eq. (5)) which is in close agreement with the previously derived value $B_0 = 13.84 \pm 0.16$ G.

The geometric phases obtained from the opposite-rotation data are plotted in Fig. 6 against the angle between flippers F_1 and F_2. The straight line through the data points represents the best fit.

Another somewhat less accurate determination of k was made from each intensity pattern $I_{yy}(\delta\beta)$ for fixed translations δx of the flipper F_2. Averaging the results of all these 13 least-squares fits to the experimental scans plotted in Fig. 4, we obtain a value $k = 1.029 \pm 0.016$. The weighted mean of these two differently derived results finally yields $k_{exp} = 0.991 \pm 0.007$.

In order to eliminate the dynamical phase contamination $\Delta\Phi_D$, the experiment was repeated by placing the flippers within a 'field-free' soft magnetic box [24]. The intensity patterns $I_{yy}(\delta\beta/2)$ recorded for parallel and opposite rotations $\delta\beta/2$ of the flippers F_1 and F_2, are converted to the fractional polarization $P_y(\delta\beta/2)/P_y(0)$ and plotted in Fig. 7. The curve for parallel-rotation remains flat as expected for the null geometric phase, while the opposite-rotation curve oscillates cosinusoidally due to the concomitant geometric phase. The corresponding geometric phases extracted from the raw data for opposite rotations are displayed in Fig. 7 as a function of the flipper rotations. These phases conform to theory ($k = 0.984 \pm 0.011$) very closely.

The observed geometric as well as dynamical phases are thus within about 1% of theoretical predictions. This represents a marked improvement over the agreement level of about 23% achieved previously in an interferometric experiment [20]. The improved precision has resulted primarily from the inherent advantages of the neutron polarimetric method.

In summary, we have performed a neutron polarimetric experiment observing well demarcated geometric and dynamical phases, arising respectively from a relative rotation and a relative translation between two π flippers. The results agree with theory to within about 1%.

Acknowledgements

The technical assistance of Dr. Petra Riedler during the field-free measurements is gratefully acknowledged. This work was supported by the Austrian Science Foundation (Project 10969-PHY).

References

[1] M.V. Berry, Proc. R. Soc. (London) A 392 (1984) 45.
[2] Y. Aharonov, J. Anandan, Phys. Rev. Lett. 58 (1987) 1593.
[3] J. Samuel, R. Bhandari, Phys. Rev. Lett. 60 (1988) 2339.
[4] R. Bhandari, J. Samuel, Phys. Rev. Lett. 60 (1988) 1211.
[5] S. Pancharatnam, Proc. Indian Acad. Sci. A 44 (1956) 247.
[6] J.E. Avron, A. Raveh, B. Zur, Rev. Mod. Phys. 60 (1988) 873.
[7] A.G. Wagh, V.C. Rakhecha, J. Phys. A: Math. Gen. 32 (1999) 5167.
[8] A. Shapere, F. Wilczek (Eds.), Geometric Phases in Physics, World Scientific, Singapore, 1989.
[9] M. Berry, Phys. Today 43 (1990) 34.
[10] J.W. Zwanziger, M. Koenig, A. Pines, Ann. Rev. Phys. Chem. 41 (1990) 601.
[11] J. Anandan, Nature 360 (1992) 307.
[12] A.G. Wagh, V.C. Rakhecha, Prog. Part. Nucl. Phys. 37 (1996) 485.
[13] G. Badurek, H. Rauch, D. Tuppinger, Phys. Rev. A 34 (1986) 2600.
[14] A.G. Wagh, V.C. Rakhecha, Phys. Lett. A 148 (1990) 17.
[15] A.G. Wagh, V.C. Rakhecha, in: R. Inguva (Ed.), Recent

Developments in Quantum Optics, Plenum, New York, 1993, p. 117.
[16] A. Tomita, R. Chiao, Phys. Rev. Lett. 57 (1986) 937.
[17] T. Bitter, B. Dubbers, Phys. Rev. Lett. 59 (1987) 251.
[18] D.J. Richardson, A.I. Kilvington, K. Green, S.K. Lamoreaux, Phys. Rev. Lett. 61 (1988) 2030.
[19] A.G. Wagh, Phys. Lett. A 146 (1990) 369.
[20] A.G. Wagh, V.C. Rakhecha, J. Summhammer, G. Badurek, H. Weinfurter, B.E. Allman, H. Kaiser, K. Hamacher, D.L. Jacobson, S.A. Werner, Phys. Rev. Lett. 78 (1997) 755.
[21] B.E. Allman, H. Kaiser, S.A. Werner, A.G. Wagh, V.C. Rakhecha, J. Summhammer, Phys. Rev. A 56 (1997) 4420.
[22] A.G. Wagh, V.C. Rakhecha, Phys. Lett. A 197 (1995) 112.
[23] G. Badurek, H. Weinfurter, R. Gähler, A. Kollmar, S. Wehinger, A. Zeilinger, Phys. Rev. Lett. 71 (1993) 307.
[24] G. Badurek, J. Phys. Soc. Jpn. 65 (1996) 60, Suppl. A.